of the events resulting from a chromosomal truncation. This suggests that age-induced LOH is the result of an age-dependent increase in DNA double-strand breaks and/or a decrease in the normal repair of such damage.

Complete pedigree analysis also allowed us to determine whether LOH events occurred in mother or daughter cells. The continuous appearance of colored daughter colonies in a mother's life-span demonstrated that the mother cell had undergone LOH (e.g., Fig. 1B, mother 39). A completely colored daughter colony followed by daughter colonies with wild-type cells indicated that LOH occurred in the daughter cell only, while the mother remained heterozygous (e.g., Fig. 1B, mother 28). We presumed that BIR events would occur with equal likelihood in mother and daughter cells. In contrast to this expectation, we found a strong daughter bias (nearly 20-fold) for age-induced LOH at both the *MET15* and *SAM2* loci (Fig. 2C). This asymmetry presents an interesting biological situation for the mother cell, which may be viewed as a type of stem cell (*22*, *23*). When age-induced LOH occurs, the genomic integrity of the mother appears to be maintained relative to the daughter, preserving the potential to produce subsequent daughters with a wild-type genome.

What defect causes age-induced LOH? Our mechanistic characterization allows us to eliminate several possibilities. Nondisjunction, leading to chromosome loss, is not responsible. Telomere length is not affected by replicative age in *S. cerevisiae* (*24*), precluding telomere loss as the cause of chromosomal instability. An increase in interchromosomal fusions, resulting in dicentric chromosomes, could produce substrates for BIR, but such events do not explain the daughter bias of age-induced LOH.

Rather, we postulate that aging mother cells accumulate damaged proteins over time (*25*), which effectively eliminates the normal function of a gene product required for genome integrity. This defect appears to thwart normal DNA damage detection, because, unlike young cells repairing an induced double-strand break (*26*), mother cell divisions producing a daughter with LOH lacked noticeable cell cycle delays or arrests (Fig. 1B).

The daughter bias of age-induced LOH may be the result of broken chromosomes that persist immediately after cell division. If the centromere-containing and acentric fragments are partitioned into separate nuclei, with the acentric fragment tending to remain in the mother cell (*27*), repair from the homolog by BIR (accompanied by LOH) will become the primary DNA repair option in the daughter cell.

Our results provide predictions about the mechanisms that underlie age-related genomic instability in eukaryotic cells, as well as a model system in which to test them. Ultimately, deeper understanding of this phenomenon in yeast may help to solve the link between oncogenesis and age in humans.

References and Notes

1. R. A. DePinho, *Nature* **408**, 248 (2000).
2. P. C. Nowell, *Science* **194**, 23 (1976).
3. A. Morley, *Ann. N.Y. Acad. Sci.* **854**, 20 (1998).
4. G. Acuña, F. Würgler, C. Sengstag, *Environ. Mol. Mutagen.* **24**, 307 (1994).
5. F. Paques, J. E. Haber, *Microbiol. Mol. Biol. Rev.* **63**, 349 (1999).
6. A. Aguilera, S. Chavez, F. Malagon, *Yeast* **16**, 731 (2000).
7. *Saccharomyces* Genome Database (available at http://www.yeastgenome.org/).
8. H. Roman, *Cold Spring Harbor Symp. Quant. Biol.* **21**, 175 (1956).
9. G. J. Cost, J. D. Boeke, *Yeast* **12**, 939 (1996).
10. R. Mortimer, J. Johnston, *Nature* **183**, 1751 (1959).
11. Materials and methods are available as supporting material on *Science* Online.
12. D. A. Sinclair, L. Guarente, *Cell* **91**, 1033 (1997).
13. P. A. Defossez *et al.*, *Mol. Cell* **3**, 447 (1999).
14. M. Kaeberlein, M. McVey, L. Guarente, *Genes Dev.* **13**, 2570 (1999).
15. M. A. McMurray, D. E. Gottschling, unpublished data.
16. S. Gottlieb, R. E. Esposito, *Cell* **56**, 771 (1989).
17. S. M. Jazwinski, *Mech. Ageing Dev.* **122**, 865 (2001).
18. S. Fogel, D. D. Hurst, *Genetics* **48**, 321 (1963).
19. F. K. Zimmermann, *Mutat. Res.* **31**, 71 (1975).
20. S. R. Judd, T. D. Petes, *Genetics* **118**, 401 (1988).
21. E. Kraus, W.-Y. Leung, J. E. Haber, *Proc. Natl. Acad. Sci. U.S.A.* **98**, 8255 (2001).
22. S. A. Frank, Y. Iwasa, M. A. Nowak, *Genetics* **163**, 1527 (2003).
23. J. Cairns, *Proc. Natl. Acad. Sci. U.S.A.* **99**, 10567 (2002).
24. N. P. D'Mello, S. M. Jazwinski, *J. Bacteriol.* **173**, 6709 (1991).
25. H. Aguilaniu, L. Gustafsson, M. Rigoulet, T. Nystrom, *Science* **299**, 1751 (2003).
26. L. L. Sandell, V. A. Zakian, *Cell* **75**, 729 (1993).
27. A. W. Murray, J. W. Szostak, *Cell* **34**, 961 (1983).

28. We thank D. Andersen, S. Biggins, R. G. Gardner, F. van Leeuwen, T. Reis, G. R. Smith, A. E. Stellwagen, and M. C. Yao for critical reading of the manuscript and B. J. Brewer for insight and advice. Supported by an NSF predoctoral fellowship to M.A.M. and by a National Institutes of Health grant (no. GM43893) and an Ellison Medical Foundation Senior Scholar Award to D.E.G.

Supporting Online Material

www.sciencemag.org/cgi/content/full/301/5641/1908/DC1
Materials and Methods
Fig. S1
Tables S1 and S2
References and Notes

6 June 2003; accepted 6 August 2003

Essential Roles for Ecdysone Signaling During *Drosophila* Mid-Embryonic Development

Tatiana Kozlova*† and Carl S. Thummel

Although functions for the steroid hormone ecdysone during *Drosophila* metamorphosis have been well established, roles for the embryonic ecdysone pulse remain poorly understood. We show that the EcR-USP ecdysone receptor is first activated in the extraembryonic amnioserosa, implicating this tissue as a source of active ecdysteroids in the early embryo. Ecdysone signaling is required for germ band retraction and head involution, morphogenetic movements that shape the first instar larva. This mechanism for coordinating morphogenesis during *Drosophila* embryonic development parallels the role of ecdysone during metamorphosis. It also provides an intriguing parallel with the role of mammalian extraembryonic tissues as a critical source of steroid hormones during embryonic development.

Ecdysone triggers the programmed cell death of obsolete larval tissues and signals cell shape changes in the imaginal discs during *Drosophila* metamorphosis, transforming the body plan of the insect from a crawling larva into an adult fly. ("Ecdysone" in this paper refers to physiologically active ecdysteroids.) Ecdysone signaling is mediated by a heterodimer of two nuclear receptors, EcR (NR1H1) and the *Drosophila* RXR ortholog USP (Ultraspiracle, NR2B4) (*1*). Characterization of *EcR* and *usp* mutants at the onset of metamorphosis has revealed similar lethal phenotypes, indicating that these factors act together to transduce the hormone signal (*1*). A high titer ecdysone pulse also occurs midway through embryonic development, peaking during germ band retraction (GBR) (*2*). GBR, dorsal closure (DC), and head involution (HI) compose the major morphogenetic movements that form the body plan of the first instar larva. Ecdysone is required for cuticle deposition during late embryogenesis (*3*, *4*), but functions for ecdysone at earlier stages of embryo-

Howard Hughes Medical Institute, Department of Human Genetics, University of Utah School of Medicine, 15 North 2030 East Room 5100, Salt Lake City, UT 84112–5331, USA.

*To whom correspondence should be addressed. E-mail: tkozlova@cas.usf.edu

†Present address: Department of Biology, University of South Florida, 4202 East Fowler Avenue, Tampa, FL 33620, USA.

genesis have been difficult to assess because ecdysteroids, as well as *EcR* mRNA and protein, are deposited maternally (*3*, *5*). *EcR* zygotic null mutants die during embryogenesis with minor cuticular defects (*6*), and germline clones of *EcR* null mutants arrest during oogenesis, resulting in female sterility (*7*).

Immunofluorescent staining with common region and isoform-specific antibodies revealed that both EcR and USP are widely expressed throughout embryogenesis (fig. S1). To investigate when these receptors are activated, we used the GAL4-LBD (ligand binding domain) system, which accurately reflects ecdysone signaling through EcR-USP at the onset of metamorphosis (*8*). *hs-GAL4-EcR* or *hs-GAL4-USP* was combined with a GAL4-dependent nuclear *lacZ* reporter gene (*UAS-nlacZ*) to determine when and where the GAL4-LBD fusion protein can be activated by its ligand in the embryo. No activation was seen at stage 11, when the germ band is completely extended and the ecdysone titer is low (Fig. 1, A and D) (*2*). Activation was first evident at stage 12, when GBR begins, and was high at stage 13 (Fig. 1, B and E), when the ecdysone titer peaks, the germ band is retracted, and the dorsal surface of the embryo is covered by the amnioserosa. GAL4-EcR and GAL4-USP displayed similar patterns of activation, first detectable in the amnioserosa and remaining high in this tissue through the completion of DC at stages 14 and 15 (Fig. 1, C and F). More widespread activation was seen at later stages of embryogenesis (Fig. 1, C and F) (*9*). Endogenous EcR-USP activation was determined using a multimerized *hsp27* Ecdysone Response Element driving *lacZ* expression (*7xEcRE-lacZ*) (*5*), although other nuclear receptors can also bind to this EcRE. The pattern of *7xEcRE-lacZ* expression was similar to that of GAL4-EcR and GAL4-USP in the amnioserosa and was detectable in other tissues at stages 13 and 14 (Fig. 1, G to I). These observations are consistent with the specific and transient high-level expression of another ecdysone-dependent reporter, *DR3-Fbp-1-lacZ*, in the amnioserosa at stages 12 and 13 (*10*). As a control, we used antibodies against GAL4 to show that GAL4-EcR and GAL4-USP are widely expressed in both the amnioserosa and epidermis at stages 11 to 13. In addition, *hs-GAL4* can drive strong uniform expression of β-galactosidase at stage 9, which persisted into stages 11 to 15 (*9*). Finally, embryos cultured with exogenous 20-hydroxyecdysone, a physiologically active ecdysteroid, displayed efficient and widespread *7xEcRE-lacZ* expression at stage 9 (Fig. 2), when EcR-USP is normally silent (Fig. 1). Taken together, these observations indicate that the amnioserosa contains a high concentration of active ecdysteroids during mid-embryogenesis.

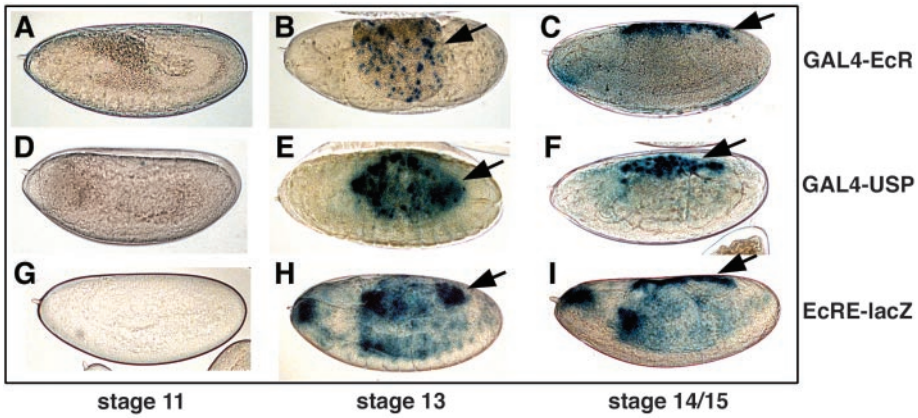

Fig. 1. The ecdysone receptor is activated in the amnioserosa. Histochemical staining for β-galactosidase expression in heat-treated *hs-GAL4-EcR*/+; *UAS-nlacZ*/+ (**A** to **C**), *hs-GAL4-USP*/+; *UAS-nlacZ*/+ (**D** to **F**), or *7xEcRE-lacZ* (**G** to **I**) embryos is shown. Activation was not detectable at stage 11 (A, D, and G), before the ecdysone pulse, but was strong in the amnioserosa at stage 13 [(B), (E), and (H), arrows], persisting through stages 14 and 15 [(C), (F), and (I), arrows]. Longer histochemical staining of these later stage embryos revealed widespread activation outside of the amnioserosa (*9*). All embryos are oriented anterior to the left and dorsal side up, except for (B), (E), and (H), where the embryos are shown from a dorsal-lateral perspective. The activation pattern in the amnioserosa of stage 13 *7xEcRE-lacZ* embryos was most intense at the anterior and posterior ends of this tissue [(H), arrow points to posterior patch], similar to the pattern of GAL4-USP [(E), arrow], but more pronounced. Activation in the amnioserosa was uniform at stage 14 and 15 in all genotypes [(C), (F), (I), arrows]. Patterns shown were consistent among several hundred embryos examined.

The amnioserosa is an extraembryonic tissue that does not contribute to the embryo proper, but which is nevertheless essential for both GBR and DC (*11*–*13*). To test whether ecdysone signaling is required for these morphogenetic events, we inactivated both maternal and zygotic *EcR* functions by expressing either of two different dominant-negative *EcR* constructs during early embryogenesis: *hs-GAL4-EcR* or *UAS-EcR-F645A* (*8*, *14*). As an independent means of disrupting ecdysone signaling, we used a temperature-sensitive ecdysone-deficient mutant, *ecd1* (*15*), under conditions where both maternal and zygotic ecdysone levels are reduced. Expression of an *EcR* dominant-negative construct, or maintaining *ecd1* mutants at a nonpermissive temperature, resulted in embryonic lethality (Fig. 3A) with highly penetrant defects in GBR, HI, and cuticle deposition (Fig. 3B). Weak GBR defects included malformed mouthhooks and a dorsal shift in the position of the posterior spiracles (Fig. 3D), whereas stronger phenotypes included a complete block in GBR and an anterior cuticular hole, indicating defective HI (Fig. 3E). No *ecd1* mutant embryos arrested development before GBR, suggesting that this is the earliest embryonic function for ecdysone. Embryonic lethality caused by heat-treating *hs-GAL4-EcR*/+ embryos at 3 to 5 hours after egg laying increased from 60 to 96% in a heterozygous *EcR* mutant background, indicating that this dominant-negative construct interfered with endogenous *EcR* function. Both the penetrance and expressivity of the GBR defect also increased under these conditions (*16*). To determine whether ecdysone signaling is required in the amnioserosa and/or the germ band for GBR, we expressed *UAS-EcR-F645A* under the control of the amnioserosa-specific GAL4 drivers *C381*

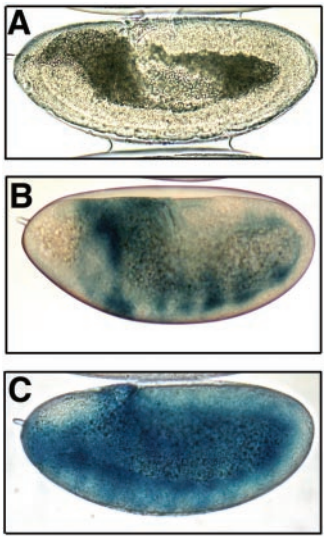

Fig. 2. Widespread activation of the ecdysone receptor in embryos cultured with 20-hydroxyecdysone (20E). Zero- to 4-hour *7xEcRE-lacZ* embryos were cultured with 5×10^{-6} M 20E or with vehicle control (1% ethanol) and histochemically stained for β-galactosidase expression. Sixty percent ($n = 67$) of the embryos cultured in the presence of 20E showed premature and widespread *7xEcRE-lacZ* expression at stages 9 to 11, ranging from (**B**) moderate to (**C**) high expression. (**A**) Control embryos showed no activation ($n = 88$). Embryos are oriented anterior to the left and dorsal side up.

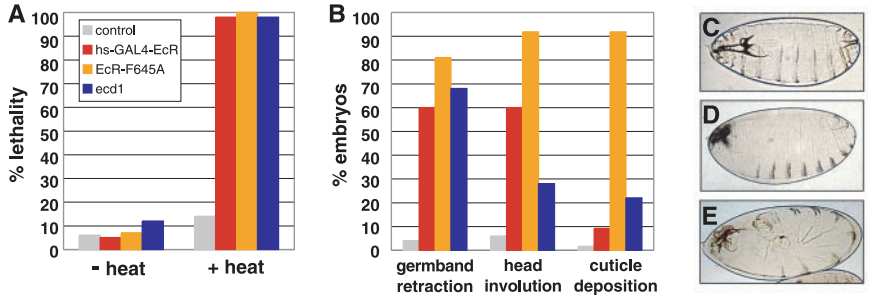

Fig. 3. Ecdysone signaling is required for germ band retraction, head involution, and cuticle deposition. (**A** and **B**) w^{1118} (control), *hs-GAL4-EcR*, or *hs-GAL4/+*; *UAS-EcR-F645A/+* (*EcR-F645A*) embryos were maintained at either 25°C (– heat) or heat-treated at 3 to 5 hours after egg laying (+ heat). Embryos from *ecd1* mutant flies maintained at either the permissive (– heat) or nonpermissive (+ heat) temperature were also analyzed for either lethality (A) (n = 200 to 300 in at least two independent experiments) or embryonic lethal phenotypes (B) (n = 100 to 120) (*16*). (**C** to **E**) The lethal phenotypes of embryos expressing the GAL4-EcR dominant-negative range from relatively mild defects in GBR and HI (D) to a strong block in these morphogenetic pathways (E), in comparison to a control w^{1118} embryo (C).

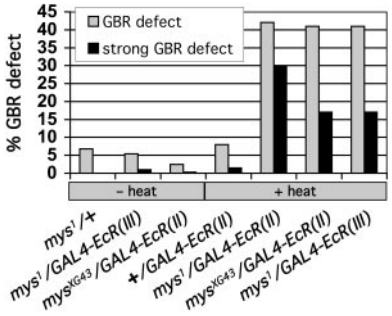

Fig. 4. Functional interaction between ecdysone signaling and βPS integrin in germ band retraction. Embryos from the respective crosses (*16*) were maintained at either 25°C or heat-treated at 3 to 5 hours after egg laying. The penetrance of total GBR defects (weak + strong) and strong GBR defects (fully extended germ band) are depicted. Forty to 80 embryos were examined for each genotype. A single copy of the GAL4-EcR dominant negative construct alone [*+/GAL4-EcR(II)*] generated relatively weak GBR defects in this experiment because two copies of the transgene are required to produce the strong phenotypes shown in Fig. 3.

and *LP-1* or the ectodermal-specific GAL4 driver *69B*. These crosses led to embryonic and first instar larval lethality with low-penetrance GBR defects (*9*). Upon repeating these experiments in a sensitized *EcR* genetic background, 23 and 15% of the embryos that express *UAS-EcR-F645A* under control of *69B-GAL4* or *C381-GAL4*, respectively, displayed GBR defects; no GBR defects were detected in control embryos (*16*). Thus, ecdysone signaling appears to be required in both the amnioserosa and germ band for GBR to proceed. Mutations in several genes that are required for GBR (*Egfr*, *hnt*, *srp*, and *ush*) cause premature amnioserosa cell death (*11*, *12*, *17*). We observed a similar effect when ecdysone signaling was downregulated; however, GBR defects were observed at the same penetrance when we expressed the GAL4-EcR dominant negative in a *Df(3)H99* mutant background to block embryonic cell death (*16*). Therefore, as was shown in studies of the amnioserosa-specific Hindsight transcription factor (*18*), more than amnioserosa cell survival is required for GBR to occur.

Earlier studies have demonstrated that the amnioserosa promotes GBR through integrin-mediated adhesion to the adjacent germ band, with the highest penetrance GBR defects observed in mutants lacking both maternal and zygotic βPS integrin, encoded by *myospheroid* (*mys*) (*19*, *20*). Both the penetrance and expressivity of GBR defects were greatly enhanced when the *hs-GAL4-EcR* dominant negative was expressed in embryos that carry a reduced dose of *mys*, but not in control embryos, suggesting that ecdysone exerts its effects on GBR, at least in part, through integrins (Fig. 4).

The embryonic ecdysone titer begins to rise before the formation of the ring gland, the endocrine organ of the insect, suggesting that maternally deposited ecdysteroids contribute to the embryonic ecdysone pulse (*2*, *3*). This is consistent with the maternal effect that we observe in our *ecd1* studies, where a cross of *ecd1* mutant females to wild-type males results in a high degree of GBR and HI defects in the offspring (*16*). Maternal ecdysteroids are stored as inactive conjugates in the yolk, which lies in close apposition to the amnioserosa (*21*, *22*). We propose that these inactive ecdysteroids are converted into active forms of the hormone by enzymes that reside in the yolk and/or amnioserosa, resulting in a high concentration of active ecdysteroids in the amnioserosa, defining this tissue as a critical source of the hormone.

Mutations in *dib* and *sad*, genes that encode key cytochrome P-450s in the zygotic ecdysone biosynthetic pathway, have established a role for ecdysone signaling in HI, DC, and cuticle deposition (*4*, *23*). Although we do not see penetrant DC defects when we disrupt ecdysone signaling, it is possible that this phenotype is masked by the earlier defect in GBR. Indeed, 5 to 8% of *ecd1* mutant embryos, or embryos expressing *EcR-F645A*, display an anterior-dorsal hole that could be indicative of a DC defect (*16*). Alternatively, the absence of GBR defects in *dib* and *sad* mutants may be attributed to their exclusively zygotic function and the apparent dependence of GBR on maternally contributed ecdysteroids. Finally, although our functional studies support a key role for *EcR* in mid-embryonic morphogenetic movements, reduction of maternal and zygotic *usp* function results in embryonic lethality with minor cuticle defects and no reported defects in morphogenesis (*24*, *25*). This could be due to the hypomorphic nature of two *usp* alleles used in these studies (*26*). Alternatively, EcR might exert its roles in embryonic morphogenesis independently of USP.

Two models have been proposed to explain the role of the amnioserosa in GBR, either as a source of one or more diffusible signals that trigger cell shape changes in the adjacent germ band (*18*) or through dorsoventral contraction of the amnioserosa promoting GBR via integrin-mediated adhesion between these tissues (*19*, *22*). Our results unify these models by implicating ecdysone as a critical signal from the amnioserosa that is required for GBR, as well as suggesting that ecdysone directs this response through integrins. The observation that ecdysone signaling is required in both the amnioserosa and germ band for GBR suggests that the amnioserosa may not provide all of the force for this morphogenetic event and that ecdysone-triggered cell shape changes in the germ band may also contribute to GBR. Moreover, analogous ecdysone-triggered cell shape changes drive imaginal disc morphogenesis during metamorphosis (*22*, *27*), with at least part of this genetic program required for GBR and HI during embryonic development (*28*). Genetic interactions between EcR and integrin subunits, including βPS integrin, have also been observed during adult wing morphogenesis during metamorphosis (*29*). Taken together, these observations raise the intriguing possibility that ecdysone functions in a parallel manner during embryogenesis and metamorphosis, triggering coordinated changes in cell shape that establish the basic body plan for the next phase in the life cycle. An endocrine signal in embryos also provides a mechanism to explain the temporal coordination of mid-embryonic morphogenetic events, defining a new ecdysone-dependent phase in the insect life cycle. Finally, this study provides a parallel with the function of mammalian extraembryonic tissues, where the placenta acts as a critical source of steroid hormones for the maintanence of pregnancy.

References and Notes

1. L. M. Riddiford, P. Cherbas, J. W. Truman, *Vitam. Horm.* **60**, 1 (2001).
2. P. Maroy, G. Kaufmann, A. Dubendorfer, *J. Insect Physiol.* **34**, 633 (1988).

3. J. A. Hoffmann, M. Lagueux, in *Comprehensive Insect Physiology, Biochemistry, and Pharmacology*, G. A. Kerkut, L. I. Gilbert, Eds. (Pergamon Press, Oxford, 1985), pp. 435–460.
4. V. M. Chavez, *et al.*, *Development* **127**, 4115 (2000).
5. W. S. Talbot, E. A. Swyryd, D. S. Hogness, *Cell* **73**, 1323 (1993).
6. M. Bender, F. B. Imam, W. S. Talbot, B. Ganetzky, D. S. Hogness, *Cell* **91**, 777 (1997).
7. M. Buszczak *et al.*, *Development* **126**, 4581 (1999).
8. T. Kozlova, C. S. Thummel, *Development* **129**, 1739 (2002).
9. T. Kozlova, C. S. Thummel, data not shown,
10. C. Antoniewski, B. Mugat, F. Delbac, J. A. Lepesant, *Mol. Cell. Biol.* **16**, 2977 (1996).
11. L. H. Frank, C. Rushlow, *Development* **122**, 1343 (1996).
12. M. L. Yip, M. L. Lamka, H. D. Lipshitz, *Development* **124**, 2129 (1997).
13. D. P. Kiehart, C. G. Galbraith, K. A. Edwards, W. L. Rickoll, R. A. Montague, *J. Cell. Biol.* **149**, 471 (2000).
14. L. Cherbas, X. Hu, I. F. Zhimulev, E. Belyaeva, P. Cherbas, *Development* **130**, 271 (2003).
15. A. Garen, L. Kauvar, J.-A. Lepesant, *Proc. Natl. Acad. Sci. U.S.A.* **74**, 5099 (1977).
16. Materials and methods are available as supporting material on *Science* Online.
17. R. Clifford, T. Schupbach, *Development* **115**, 853 (1992).
18. M. L. Lamka, H. D. Lipshitz, *Dev. Biol.* **214**, 102 (1999).
19. F. Schöck, N. Perrimon, *Genes Dev.* **17**, 597 (2003).
20. C. E. Roote, S. Zusman, *Dev. Biol.* **169**, 322 (1995).
21. M. Bownes, A. Shirras, M. Blair, J. Collins, A. Coulson, *Proc. Natl. Acad. Sci. U.S.A.* **85**, 1554 (1988).
22. F. Schöck, N. Perrimon, *Dev. Biol.* **248**, 29 (2002).
23. J. T. Warren *et al.*, *Proc. Natl. Acad. Sci. U.S.A.* **99**, 11043 (2002).
24. N. Perrimon, L. Engstrom, A. P. Mahowald, *Genetics* **111**, 23 (1985).
25. A. E. Oro, M. McKeown, R. M. Evans, *Development* **115**, 449 (1992).
26. N. Ghbeish *et al.*, *Proc. Natl. Acad. Sci. U.S.A.* **98**, 3867 (2001).
27. L. von Kalm, D. Fristrom, J. Fristrom, *BioEssays* **17**, 693 (1995).
28. R. E. Ward, J. Evans, C. S. Thummel, *Genetics*, in press.
29. P. P. D'Avino, C. S. Thummel, *Dev. Biol.* **220**, 211 (2000).

30. We thank D. Brower, D. Hogness, A. Letsou, H. Lipshitz, F. Schöck, and the Bloomington Stock Center for fly stocks; D. Hogness for EcR antibodies; L. Cherbas for the *UAS-EcR-F645A* transformant; members of the Thummel lab, K. Clark, and A. Letsou for discussions and suggestions in the course of this work; and A. Bashirullah, A. Letsou, and R. Ward for critical comments on the manuscript. T.K. was a Research Associate and C.S.T. is an Investigator with the Howard Hughes Medical Institute.

Supporting Online Material
www.sciencemag.org/cgi/content/full/1087419/DC1
Fig. S1
Materials and Methods
References

30 May 2003; accepted 21 August 2003
Published online 4 September 2003;
10.1126/science.1087419
Include this information when citing this paper.

Sequence-Dependent Pausing of Single Lambda Exonuclease Molecules

Thomas T. Perkins,[1]*‡ Ravindra V. Dalal,[2] Paul G. Mitsis,[3]† Steven M. Block[1,4]

Lambda exonuclease processively degrades one strand of duplex DNA, moving 5′-to-3′ in an ATP-independent fashion. When examined at the single-molecule level, the speeds of digestion were nearly constant at 4 nanometers per second (12 nucleotides per second), interspersed with pauses of variable duration. Long pauses, occurring at stereotypical locations, were strand-specific and sequence-dependent. Pause duration and probability varied widely. The strongest pause, GGCGAT TCT, was identified by gel electrophoresis. Correlating single-molecule dwell positions with sequence independently identified the motif GGCGA. This sequence is found in the left lambda cohesive end, where exonuclease inhibition may contribute to the reduced recombination efficiency at that end.

Exonucleases are integral components of many genetic repair and recombination pathways (*1*). Processive 5′→3′ exonucleases generate DNA intermediates with long 3′-overhangs involved in these pathways (*1*, *2*); in bacteriophage lambda, the Red α gene encodes the 24-kD subunit of such a nuclease (*3*). The structure of lambda exonuclease (λ-exo) consists of a toroidal homotrimer of subunits, with a tapered central channel sufficient to admit double-stranded DNA (dsDNA) at its entrance but only wide enough to pass single-stranded DNA (ssDNA) through its exit (*4*). A topological constraint may therefore underlie the high processivity of λ-exo (>3000 base pairs, where 1 bp corresponds to a helical rise of 0.338 nm along dsDNA) (*5*). λ-exo digestion requires Mg^{2+}, but does not require ATP or GTP, and proceeds along DNA at rates of 2 to 3.5 nm/s, as determined by bulk biochemical studies (*6*, *7*).

Here, we developed a novel high-resolution, single-molecule assay to study λ-exo motion by optical trapping nanometry. Besides measuring individual translocation rates, single-molecule studies provide insights into other processes that

[1]Department of Biological Sciences, [2]Department of Physics, and [4]Department of Applied Physics, Stanford University, Stanford, CA 94305, USA. [3]Praelux, Inc., Lawrenceville, NJ 08646, USA.

*Present address: JILA, National Institute of Standards and Technology and University of Colorado, Boulder, CO 80309–0440, USA.
†Present address: Amersham Biosciences, 800 Centennial Road, Piscataway, NJ 08855, USA.
‡To whom correspondence should be addressed. E-mail: tperkins@jila.colorado.edu

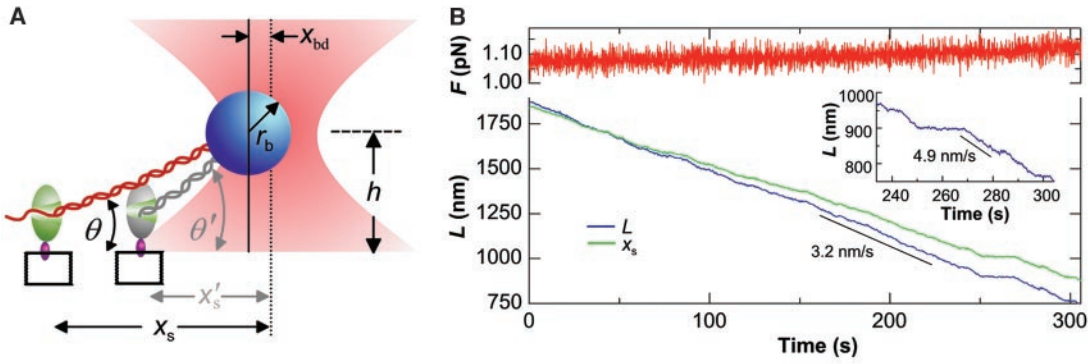

Fig. 1. (**A**) Experimental geometry of the stage-based optical force clamp (not to scale); bead displacement relative to the trap center (x_{bd}) was maintained by stage motions ($x_s \rightarrow x_s'$) that kept the load constant. The bead was positioned at a predetermined height above the coverslip; $h = 200$ nm + r_b, where r_b is the bead radius. (**B**) A representative record of λ-exo digestion in force-clamp mode over 5 min, during which the enzyme moved >1 μm. (Left) Force was clamped at 1.07 pN (red) and varied <5% (the small increase is due to changes in the vertical component of the force, which depends weakly on θ). (Right) Traces of stage motion (green) and the contour length, *L*, of the dsDNA remaining (blue), showing periods of steady movement interspersed with pauses. Inset, magnified view of DNA contour length over the interval 240 to 300 s that illustrates pauses of varying lengths. Line fits over the regions of uniform motion indicated (black lines) show the average velocity.